

# SequentialPointNet: A strong frame-level parallel point cloud sequence classification network for 3D action recognition

Xing Li, Qian Huang, Zhijian Wang, Zhenjie Hou, and Tianjin Yang

**Abstract**—The point cloud sequence of 3D human actions consists of a set of ordered point cloud frames. Compared to static point clouds, point cloud sequences have huge data sizes proportional to the time dimension. Therefore, developing an efficient and lightweight point cloud sequence model is pivotal for 3D action recognition. In this paper, we propose a strong frame-level parallel point cloud sequence network referred to as SequentialPointNet for 3D action recognition. The key to our approach is to divide the main modeling operations into frame-level units executed in parallel, which greatly improves the efficiency of modeling point cloud sequences. Moreover, we propose to flatten the point cloud sequence into a new point data type named hyperpoint sequence that preserves the complete spatial structure of each frame. Then, a novel Hyperpoint-Mixer module is introduced to mix intra-frame spatial features and inter-frame temporal features of the hyperpoint sequence. By doing so, SequentialPointNet maximizes the appearance encoding ability and extracts sufficient motion information for effective human action recognition. Extensive experiments show that SequentialPointNet achieves up to  $10\times$  faster than existing point cloud sequence models. Additionally, our SequentialPointNet surpasses state-of-the-art approaches for human action recognition on both large-scale datasets (*i.e.*, NTU RGB+D 60 and NTU RGB+D 120) and small-scale datasets (*i.e.*, MSR Action3D and UTD-MHAD). SequentialPointNet’s code is available at <https://github.com/XingLi1012/SequentialPointNet.git>.

**Index Terms**—3D Action recognition, Point cloud sequence, Parallel network.

## I. INTRODUCTION

WITH the release of low-cost depth cameras, 3D human action recognition has attracted more and more attention from researchers. 3D human action recognition can be divided into three categories based on different data types: 1) skeleton sequence-based 3D human action recognition [1]–[5], 2) depth sequence-based 3D human action recognition [6]–[11], 3) point cloud sequence-based 3D human action recognition [12]–[14]. Compared with skeleton sequence-based approaches, point cloud sequences are more convenient to be collected without additional pose estimation algorithms. Compared with depth sequence-based approaches, point cloud sequence-based methods yield lower computation costs. For

these reasons, we focus on point cloud sequence-based 3D human action recognition in this work.

Point cloud sequences of 3D human actions exhibit unordered intra-frame spatial information and ordered inter-frame temporal information. Due to the complex data structures, capturing the spatio-temporal textures from point cloud sequences is extremely challenging. An intuitive way is to convert point cloud sequences to 3D point clouds and employ static point cloud methods, *e.g.*, PointNet++ [15], to process. However, using static 3D point clouds to represent the entire point cloud sequence loses a lot of spatio-temporal information, which reduces the recognition performance. Therefore, point cloud sequence methods are necessary, which directly consumes the point cloud sequence for 3D human action classification. In order to model the dynamics of point cloud sequences, cross-frame spatio-temporal local neighborhoods around the centroids are usually constructed [16]–[18]. Then, point convolution [16] or PointNet [17], [18] are used to encode the spatio-temporal local structures. However, this complex cross-frame computing may be time-consuming and is not conducive to parallel computation.

In this paper, we propose a strong frame-level parallel point cloud sequence network called SequentialPointNet. First, each point cloud frame is flattened into a hyperpoint by the same trainable hyperpoint embedding module. The hyperpoint embedding module is a kind of static point cloud technology, which designed based on PointNet. Since PointNet can arbitrarily approximate continuous functions, the hyperpoint sequence has the ability to retain complete human appearance information of each frame. Then, the Hyperpoint-Mixer module is proposed to mix features of the hyperpoint sequence. In this module, intra-frame channel-mixing operations and inter-frame frame-mixing operations are clearly separated and the frame-mixing operation is placed at the end of all feature mixing operations. Taking the frame-mixing operation as the watershed, SequentialPointNet can be divided into a front part and a back part. Since there are no cross-frame computational dependencies, the front part can be divided into frame-level units executed in parallel. Furthermore, separating the channel-mixing operations and frame-mixing operations avoids the mutual influence of temporal and spatial information extraction, which maximizes the human appearance encoding ability. Hence, SequentialPointNet also yields superior recognition accuracy for 3D human action recognition.

Our main contributions are summarized as follows:

- We propose a strong frame-level parallel point cloud se-

Manuscript received November 19, 2021. This work is supported by the Fundamental Research Funds of China for the Central Universities No. B200202188. (Corresponding author: Qian Huang.)

X. Li, Q. Huang, Z. Wang, and T. Yang are with the Key Laboratory of Water Big Data Technology of Ministry of Water Resources, Hohai University; and School of Computer and Information, Hohai University, Nanjing 211100, China (e-mail: huangqian@hhu.edu.cn).

Z. Hou is with Changzhou University.

quence classification network, dubbed SequentialPointNet, to recognize 3D human actions. The key to SequentialPointNet is to divide the main modeling operations into frame-level units executed in parallel, which greatly improves the efficiency of modeling point cloud sequences.

- In terms of our technical contribution, we propose to flatten the point cloud sequence into a new point data type named hyperpoint sequence and introduce a novel Hyperpoint-Mixer module to perform feature mixing for the hyperpoint sequence, based on which the appearance and motion information can be readily extracted for 3D human action recognition.

- Our SequentialPointNet achieves up to 10× faster than existing point cloud sequence models and yields the cross-view accuracy of 97.6% on the NTU RGB+D 60 dataset, the cross-setup accuracy of 95.4% on the NTU RGB+D 120 dataset, the cross-subject accuracy of 91.94% on the MSR Action3D dataset, and the cross-subject accuracy of 92.31% on the UTD-MHAD dataset, which outperforms the state-of-the-art methods.

## II. RELATED WORK

### A. Static Point Cloud Modeling

With the popularity of low-cost 3D sensors, deep learning on static point clouds have attracted much attention from researchers due to extensive applications ranging from object classification [19]–[23], part segmentation [24]–[28], to scene semantic parsing [29], [30]. Static point clouds modeling can be divided into volumetric-based methods [31]–[36] and point-based methods [37]–[40]. Volumetric-based methods usually voxelize a point cloud into 3D grids, and then a 3D Convolution Neural Network (CNN) is applied on the volumetric representation for classification. Point-based methods are directly performed on raw point clouds. PointNet [41] is a pioneering effort that directly processes point sets. The key idea of PointNet is to abstract each point using a set of Multi-layer Perceptrons (MLPs) and then assemble all individual point features by a symmetry function, *i.e.*, a max pooling operation. However, PointNet lacks the ability to capture local structures. Therefore, in [15], a hierarchical network PointNet++ is proposed to encode fine geometric structures from the neighborhood of each point. PointNet++ is made of several set abstraction levels. A set abstraction level is composed of three layers: sampling layer, grouping layer, and PointNet-based learning layer. By stacking several set abstraction levels, PointNet++ progressively abstracts larger and larger local regions along the hierarchy.

### B. Time Sequence Modeling

Sequential data widely exist in various research fields, such as text, audio, and video. The point cloud sequence is also a kind of sequential data. Time sequence models have been studied by the natural language processing community for decades. The emergence of Recurrent Neural Networks (RNN) [42]–[45] pushes the boundaries of time series models. Due to the capability of extracting high-dimensional features to learn complex patterns, RNN performs time-series point prediction. LSTM [46] captures the contextual representations

of words with a short memory and has additional “forget” gates to thereby overcoming both the vanishing and exploding gradient problem. GRU [47] comprises of reset gate and update gate, and handles the information flow like LSTM sans a memory unit. Transformer [48], a fully-connected attention model, models the dependency between words in the sequence. Since the model includes no recurrence and no convolution, Transformer secures the relative or absolute position within the sequence by injecting positional encoding.

### C. Point Cloud Sequence-based 3D Human Action Recognition

Point cloud sequence-based 3D human action recognition is a fairly new and challenging task. To capture spatio-temporal information from point cloud sequences, one solution is to convert point cloud sequences to 3D point clouds and employ static point cloud methods, *e.g.*, PointNet++, to process 3D point clouds. 3DV-PointNet++ [49] is the first work to recognize human actions from point cloud sequences. In 3DV-PointNet++, 3D dynamic voxel (3DV) is proposed as a novel 3D motion representation. A set of points is extracted from 3DV and input into PointNet++ for 3D action recognition in the end-to-end learning way. However, since the point cloud sequence is converted into a static 3D point cloud set, 3DV loses a lot of spatio-temporal information and increases additional computational costs.

To overcome this problem, researchers have focused mainly on investigating point cloud sequence networks that directly consume point cloud sequences for human action recognition. MeteorNet [16] is the first work on deep learning for modeling point cloud sequences. In MeteorNet, two ways are proposed to construct spatio-temporal local neighborhoods for each point in the point cloud sequence. The abstracted feature of each point is learned by aggregating the information from these neighborhoods. Fan *et al.* [17] propose a Point spatio-temporal (PST) convolution to encode the spatio-temporal local structures of point cloud sequences. PST convolution first disentangles space and time in point cloud sequences. Furthermore, PST convolutions are incorporated into a deep network namely PSTNet to model point cloud sequences in a hierarchical manner. To avoid point tracking, Point 4D Transformer (P4Transformer) network [18] is proposed to model point cloud videos. Specifically, P4Transformer consists of a point 4D convolution to embed the spatio-temporal local structures presented in a point cloud video and a Transformer to encode the appearance and motion information by performing self-attention on the embedded local features. However, in these point cloud sequence networks, cross-frame spatio-temporal local neighborhoods are usually constructed during modeling point cloud sequences, which is quite time-consuming and limits the parallel ability of networks.

## III. METHODOLOGY

In this section, a strong frame-level parallel point cloud sequence network called SequentialPointNet is proposed to recognize 3D human actions. The overall flowchart of SequentialPointNet is described in Fig. 1. SequentialPointNet contains

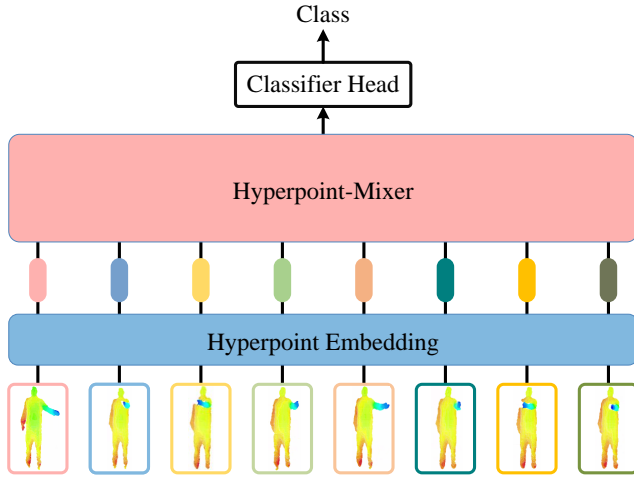


Fig. 1. SequentialPointNet contains a hyperpoint embedding module, a Hyperpoint-Mixer module, and a classifier head.

a hyperpoint embedding module, a Hyperpoint-Mixer module, and a classifier head. In Section III-A, the hyperpoint embedding module is used to flatten each point cloud frame into a hyperpoint that retains the complete human static appearance information. The intra-frame spatial features and inter-frame temporal features of the hyperpoint sequence are mixed by the Hyperpoint-Mixer module in Section III-B. In Section III-C, we analyze the frame-level parallelism of SequentialPointNet.

#### A. Hyperpoint embedding module

Recent point cloud sequence models typically construct cross-frame spatio-temporal local neighborhoods and employ point convolution or PointNet-based learning to extract spatial and temporal information. This complex cross-frame computing precludes frame-level parallelism. To avoid complex cross-frame computing, we propose to flatten each point cloud frame into a hyperpoint (also referred to as a token) by a same trainable hyperpoint embedding module. This module is employed to aggregate intra-frame geometric details and preserve them in the hyperpoint. The independent embedding of each point cloud frame enables the hyperpoint sequence to be generated in frame-level parallel. An additional advantage of this flattening operation is that superior static point cloud models can be used almost out of the box as the hyperpoint embedding module.

In the hyperpoint embedding module, each point cloud frame is flattened to a hyperpoint by static point cloud processing technology to summarize human static appearance. we first adopt the set abstraction operation twice to downsample each point cloud frame. In this process, the texture information from space partitions is aggregated into the corresponding centroids. Then, in order to characterize human entire appearance information, a PointNet layer is used. The hyperpoint embedding module is shown in Fig. 2.

The set abstraction operation in our work is made of three key layers: sampling layer, grouping layer, and augmentation PointNet layer. Specifically, let  $\mathcal{S} = \{\mathcal{S}_t\}_{t=1}^T$  denotes a point cloud sequence of  $T$  frames, and  $\mathcal{S}_t = \{x_1^t, x_2^t, \dots, x_n^t\}$

denotes the unordered point set of the  $t$ -th frame, where  $n$  is the number of points. The  $m$ -th set abstraction level takes an  $n_{m-1} \times (d + c_{m-1})$  matrix as input that is from  $n_{m-1}$  points with  $d$ -dim coordinates and  $c_{m-1}$ -dim point features. It outputs an  $n_m \times (d + c_m)$  matrix of  $n_m$  subsampled points with  $d$ -dim coordinates and new  $c_m$ -dim feature vectors summarizing local context. The size of the input in the first set abstraction level is  $n \times (d + c)$ . In this work,  $d$  is set as 3 corresponding to the 3-dim coordinate ( $X, Y, Z$ ) of each point, and  $c$  is set as 0.

In the sampling layer, farthest point sampling (FPS) is used to choose  $n_m$  points as centroids from the point set.

In the grouping layer, a point set of size  $n_{m-1} \times (d + c_{m-1})$  and the coordinates of a set of centroids of size  $n_m \times d$  are taken as input. The output is  $n_m$  groups of point sets of size  $n_m \times k_m \times (d + c_{m-1})$ , where each group corresponds to a local region and  $k_m$  is the number of local points in the neighborhood of centroid points. Ball query finds all points that are within a radius to the query point, in which an upper limit of  $k_m$  is set.

The augmentation PointNet layer in the set abstraction operation includes an inter-feature attention mechanism, a set of MLPs, and a max pooling operation. The input of this layer is  $n_m$  local regions with data size  $n_m \times k_m \times (d + c_{m-1})$ . First, the coordinates of points in a local region are translated into a local frame relative to the centroid point. Second, the distance between each local point and the corresponding centroid is used as a 1-dim additional point feature to alleviate the influence of rotational motion on action recognition. Then, an inter-feature attention mechanism is used to optimize the fusion effect of different features. The inter-feature attention mechanism is realized by Convolutional Block Attention Module (CBAM) in [50]. The inter-feature attention mechanism is not used in the first set abstraction operation due to only the 1-dim point feature. In the following, a set of MLPs are applied to abstract the features of each local point. Then, the representation of a local region is generated by incorporating the abstracted features of all local points using a max pooling operation. Finally, coordinates of the centroid point and its local region representation are concatenated as abstracted features of this centroid point. The augmentation PointNet layer is formalized as follows:

$$r_j^t = \text{MAX}_{i=1, \dots, k_m} \{ \text{MLP} ( [(l_{j,i}^t - o_j^t) \ominus e_{j,i}^t \ominus p_{j,i}^t] \odot A) \} \ominus o_j^t \quad (1)$$

where  $l_{j,i}^t$  is the coordinates of  $i$ -th point in the  $j$ -th local region from the  $t$ -th point cloud frame.  $o_j^t$  and  $p_{j,i}^t$  are the coordinates of the centroid point and the point features corresponding to  $l_{j,i}^t$ , respectively.  $e_{j,i}^t$  is the euclidean distance between  $l_{j,i}^t$  and  $o_j^t$ .  $A$  is the attention mechanism with  $(3+1+c_{m-1})$ -dim scores corresponding to the coordinates and features of each point. Attention scores in  $A$  are shared among all local points from all point cloud frames.  $\ominus$  and  $\odot$  are the concatenation operation and dot product operation, respectively.  $r_j^t$  is the abstracted features of the  $j$ -th centroid point from the  $t$ -th point cloud frame.

The set abstract operation is performed twice in the hyperpoint sequence module. In order to characterize the spatial

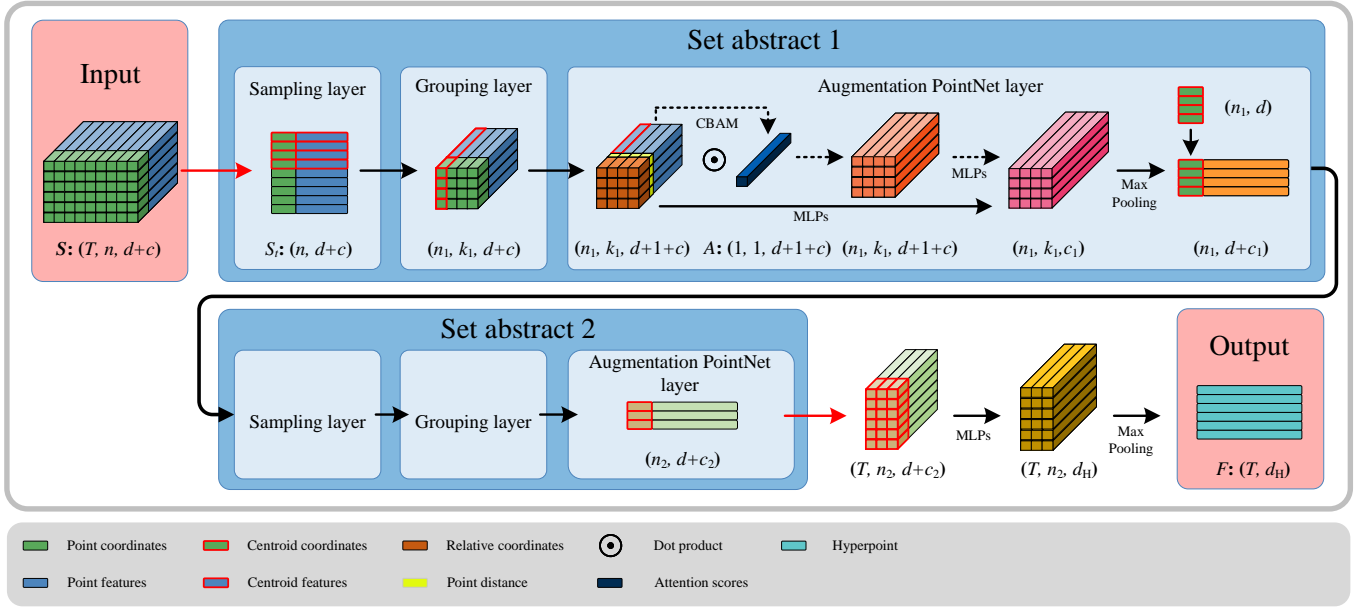


Fig. 2. The hyperpoint embedding module contains two set abstraction operation, and a PointNet layer.

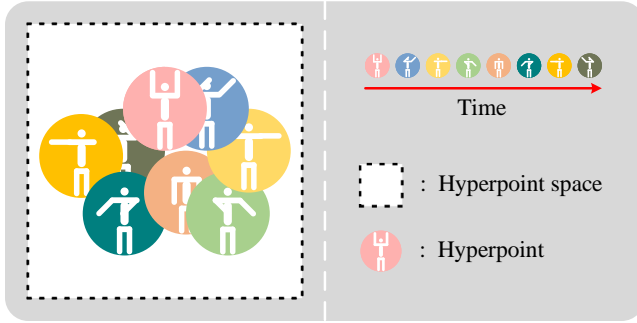


Fig. 3. The hyperpoint sequence is a set of ordered hyperpoints in the hyperpoint space, recording changing internal textures of each point cloud frame along the time dimension.

appearance information of the entire point cloud frame, a PointNet layer consisting of a set of MLPs and a max pooling operation is used as follows:

$$\mathbf{F}_t = \text{MAX}_{j=1, \dots, n_2} \{ \text{MLP}(r_j^t) \} \quad (2)$$

where  $\mathbf{F}_t$  is the hyperpoint of the  $t$ -th point cloud frame. So the hyperpoint sequence is represented as  $\mathbf{F} = \{\mathbf{F}_t\}_{t=1}^T$ .

The hyperpoint is a high-dimensional point, which is a texture summary of the static point cloud in a selected area. As shown in Fig. 3, the hyperpoint sequence is a set of ordered hyperpoints in the hyperpoint space, recording changing internal textures of each point cloud frame along the time dimension. The hyperpoint sequence is a new point data type. Adjacent hyperpoints in the hyperpoint sequence have high similarity. Compared with complex internal spatial information, the change (*i.e.*, temporal information) between hyperpoints is relatively simple.

To the best of our knowledge, we are the first to flatten the point cloud frame to a hyperpoint in point cloud sequence

models. In order to demonstrate that the hyperpoint retains the complete human static appearance information, we provide a theoretical foundation for our flattening operation by showing the universal approximation ability of the hyperpoint embedding module to continuous functions on point cloud frames.

Formally, let  $\mathcal{X} = \{S : S \subseteq [0, 1]^c \text{ and } |S| = n\}$  is the set of  $c$ -dimensional point clouds inside a  $c$ -dimensional unit cube.  $f : \mathcal{X} \rightarrow \mathbb{R}$  is a continuous set function on  $\mathcal{X}$  w.r.t to Hausdorff distance  $D_H(\cdot, \cdot)$ , *i.e.*,  $\forall \epsilon > 0, \exists \delta > 0$ , for any  $S, S' \in \mathcal{X}$ , if  $D_H(\cdot, \cdot) < \delta$ , then  $|f(S) - f(S')| < \epsilon$ . The theorem 1 [41] says that  $f$  can be arbitrarily approximated by PointNet given enough neurons at the max pooling layer.

**Theorem 1.** Suppose  $f : \mathcal{X} \rightarrow \mathbb{R}$  is a continuous set function w.r.t Hausdorff distance  $D_H(\cdot, \cdot)$ .  $\forall \epsilon > 0, \exists$  a continuous function  $h$  and a symmetric function  $g(x_1, \dots, x_n) = \gamma \circ \text{MAX}$ , such that for any  $S \in \mathcal{X}$ ,

$$\left| f(S) - \gamma \left( \text{MAX}_{x_i \in S} \{h(x_i)\} \right) \right| < \epsilon$$

where  $x_1, \dots, x_n$  is the full list of elements in  $S$  ordered arbitrarily,  $\gamma$  is a continuous function, and  $\text{MAX}$  is a vector max operator that takes  $n$  vectors as input and returns a new vector of the element-wise maximum.

As stated above, continuous functions can be arbitrarily approximated by PointNet given enough neurons at the max pooling layer. The hyperpoint embedding module is a recursive application of PointNet on nested partitions of the input point set. Therefore, the hyperpoint embedding module is able to arbitrarily approximate continuous functions on point cloud frames given enough neurons at max pooling layers and a suitable partitioning strategy. In other words, the hyperpoint embedding module is not only a frame-level parallel architecture but also has the ability to extract the complete human static appearance information from the point cloud sequence.

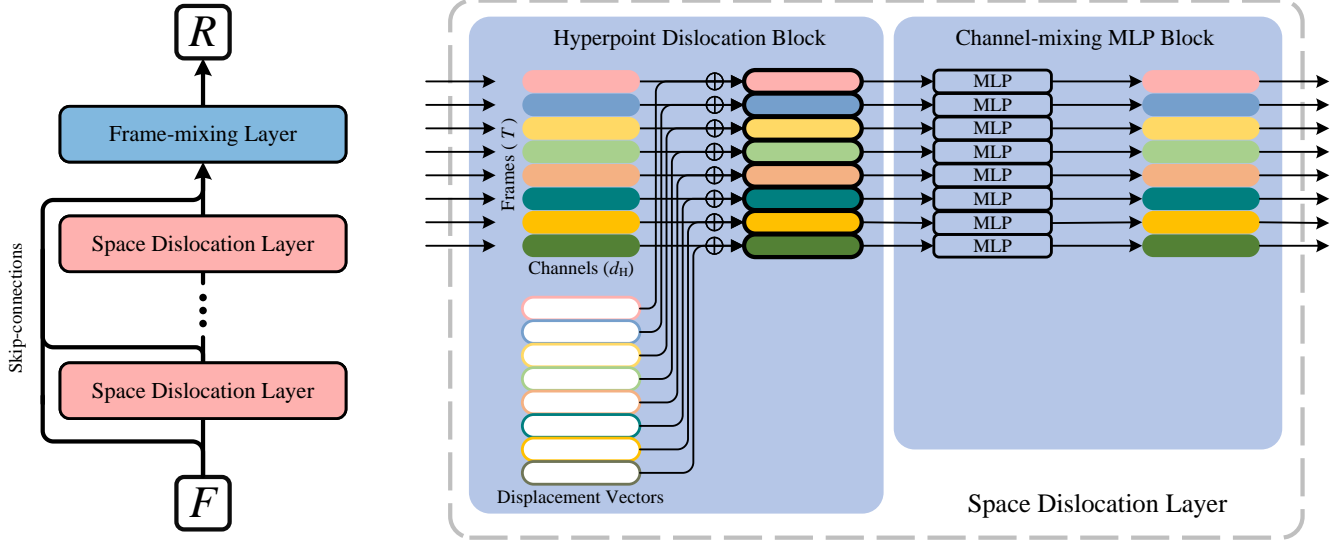


Fig. 4. Left: Hyperpoint-Mixer module. Right: Space dislocation layer. The Hyperpoint-Mixer module consists of multiple space dislocation layers of identical size, a frame-mixing layer, and a multi-level feature learning based on skip-connection operations. The space dislocation layer is composed of a hyperpoint dislocation block, and a channel-mixing MLP block.

### B. Hyperpoint-Mixer module

Hyperpoint-Mixer module is proposed to perform feature mixing of hyperpoint sequences. Existing point cloud sequence models consist of architectures that mix intra-frame spatial and inter-frame temporal features. MeteorNet, P4Transformer, and PSTNet mix spatial and temporal features at once in cross-frame spatio-temporal local neighborhoods. The idea behind the Hyperpoint-Mixer module is to (i) clearly separate the spatial (channel-mixing) operation and the temporal (frame-mixing) operation, (ii) design a frame-mixing operation of low computational complexity which is executed following the last channel-mixing operation. The intra-frame spatial information and the inter-frame temporal information in hyperpoint sequences may not be compatible. Separating the channel-mixing operations and the frame-mixing operation can avoid the mutual influence of spatial and temporal information extraction, which maximizes the human appearance encoding ability. Moreover, due to (i) and (ii), the Hyperpoint-Mixer module motivates the main operations of SequentialPointNet to execute in frame-level parallel.

Fig. 4 summarizes the Hyperpoint-Mixer module. The point cloud sequence is flattened to a hyperpoint sequence  $F \in \mathbb{R}^{T \times d_H}$  and input into the Hyperpoint-Mixer module to mix spatial and temporal features. This module consists of multiple space dislocation layers of identical size, a multi-level feature learning based on skip-connection operations, and a frame-mixing layer.

1) *Space dislocation layer*: The space dislocation layer is composed of a hyperpoint dislocation block, and a channel-mixing MLP block, which is presented to perform the intra-frame spatial feature mixing of hyperpoints in the new dislocated space. Simple symmetric functions like averaging, maximum, and addition operations are common feature aggregating

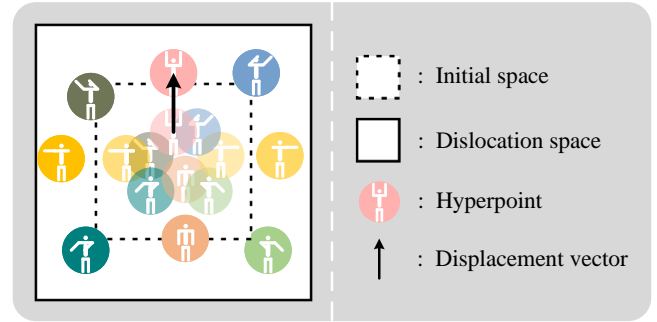


Fig. 5. In the hyperpoint dislocation block, by adding the corresponding displacement vector, hyperpoints are dislocated from the initial space to different spatial positions to record the temporal order.

matters with low computational complexity. In this paper, the symmetric function is adopted as the frame-mixing layer. However, symmetric functions are insensitive to the input order of hyperpoints. To overcome this problem, we must embed temporal information into the hyperpoint sequence. In the hyperpoint dislocation block, by adding the corresponding displacement vector, hyperpoints are dislocated from the initial space to different spatial positions to record the temporal order as shown in Fig. 5. The essence of the hyperpoint dislocation block is to convert the hyperpoint order into a coordinate component of the hyperpoint to embed temporal information. Specifically, displacement vectors are generated using the sine and cosine functions of different frequencies [48]:

$$DV_{t,2h} = \sin\left(t/10000^{2h/d_H}\right) \quad (3)$$

$$DV_{t,2h+1} = \cos\left(t/10000^{2h/d_H}\right) \quad (4)$$

where  $d_H$  denotes the number of channels.  $t$  is the temporal position and  $h$  is the dimension position. Then, the channel-mixing MLP block acts on each hyperpoint in the dislocation space to perform the channel-mixing operation, maps  $\mathbb{R}^{d_H} \rightarrow \mathbb{R}^{d_H}$ , and is shared across all hyperpoints. Each channel-mixing MLP block contains a set of fully-connected layers and ReLU non-linearities. Space dislocation layers can be formalized as follows:

$$\mathbf{F}_t^\ell = MLP(\mathbf{F}_t^{\ell-1} + DV_t), \quad \text{for } t = 1 \dots T. \quad (5)$$

where  $\mathbf{F}^\ell$  is the new hyperpoint sequences after the  $\ell$ -th space dislocation layer.

Each space dislocation layer takes an input of the same size, which is an isotropic design. With the stacking of space dislocation layers, hyperpoints are dislocated at increasingly larger scales. In the larger dislocation space, the coordinates of hyperpoints record more temporal information but less spatial information. Multi-level feature learning [51] is often used in vision tasks, which can improve recognition accuracy. In order to obtain more discriminant information, multi-level features from different dislocation spaces are added by skip-connection operations and sent into the symmetric function as follows:

$$\mathbf{R}_i = g_{t=1, \dots, T} \{(\mathbf{F} + \mathbf{F}^1 + \dots + \mathbf{F}^\ell)_{t,i}\} \quad (6)$$

where  $g: \mathbb{R}^{T \times d_H} \rightarrow \mathbb{R}^{d_H}$  is a symmetric function.  $\mathbf{R}$  is the global spatio-temporal feature of the hyperpoint sequence.

2) *Frame-mixing layer*: The frame-mixing layer is used to perform the feature mixing across frames. Since the temporal information has been injected, the max pooling operation is adopted as the frame-mixing layer to aggregate spatio-temporal information from all the hyperpoints. In order to capture the subactions within the point cloud sequence, the hierarchical pyramid max pooling operation is used, which divides the fused hyperpoint sequence  $\tilde{\mathbf{F}} = \mathbf{F} + \mathbf{F}^1 + \dots + \mathbf{F}^\ell$  into multiple temporal partitions of the equal number of hyperpoints and then performs the max pooling operation in each partition to generate the corresponding descriptors. In this work, we employ a 2-layer pyramid with three partitions. Then, the descriptors from all temporal partitions are simply concatenated to form the global spatio-temporal feature  $\mathbf{R}$ . Finally, the output of the Hyperpoint-Mixer module is input to a fully-connected classifier head for recognizing human actions.

It is worth mentioning that the Hyperpoint-Mixer module can also be viewed as a time sequence model. Compared to RNN-like and Transformer-like networks, the Hyperpoint-Mixer module implements more competitive performance on the hyperpoint sequence classification task. Different from the conventional sequential data, the internal structures of the hyperpoint generate the main discriminant information and the dynamics between the hyperpoints are auxiliary. Therefore, the time sequence models that implement strict temporal inference are not suitable for hyperpoint sequences. Channel-mixing operations and the frame-mixing operation are separated in the Hyperpoint-Mixer module, which avoids the mutual influence of temporal and spatial information extraction and maximizes the encoding ability for intra-frame human appearance. The

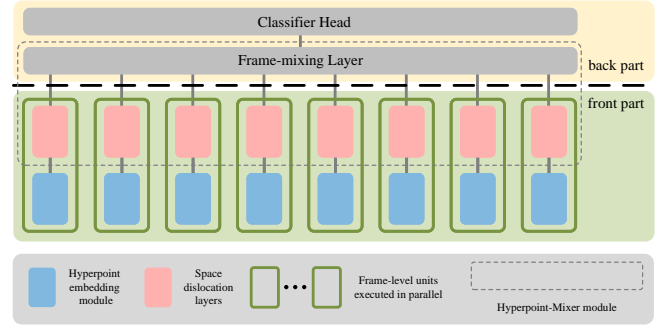


Fig. 6. The computation graph of SequentialPointNet.

symmetry function assisted by the hyperpoint dislocation block also preserves plentiful dynamic information for effective human action recognition.

### C. Frame-level parallelism

Fig. 6 demonstrates the computation graph of SequentialPointNet. Taking the frame-mixing layer as the watershed, SequentialPointNet can be divided into a front part and a back part. Since there is no cross-frame computational dependency, operations of the front part can be divided into frame-level units executed in parallel. Each frame-level unit includes a hyperpoint embedding module and all space dislocation layers. The back part only contains architectures of low computational complexity including the frame-mixing operation and a classifier head. Therefore, the main operations (*i.e.*, the front part) in SequentialPointNet can be executed in frame-level parallel, based on which the efficiency of modeling point cloud sequences is greatly improved.

## IV. EXPERIMENTS

In this section, we firstly introduce the datasets and experimental implementation details. Then, we compare our SequentialPointNet with the existing state-of-the-art methods. Again, we conduct detailed ablation studies to further demonstrate the contributions of different components in our SequentialPointNet. Finally, we compare the memory usage and computational efficiency of our SequentialPointNet with other point cloud sequence models.

### A. Datasets

We evaluate the proposed method on two large-scale public datasets (*i.e.*, NTU RGB+D 60 [52] and NTU RGB+D 120 [53]) and two small-scale public dataset (*i.e.*, MSR Action3D dataset [54] and UTD Multimodal Human Action Dataset [55] (UTD-MHAD)).

The NTU RGB+D 60 dataset is composed of 56880 depth video sequences for 60 actions and is one of the largest human action datasets. Both cross-subject and cross-view evaluation criteria are adopted for training and testing.

The NTU RGB+D 120 dataset is the largest dataset for 3D action recognition, which is an extension of the NTU RGB-D 60 dataset. The NTU RGB+D 120 dataset is composed of

114480 depth video sequences for 120 actions. Both cross-subject and cross-setup evaluation criteria are adopted for training and testing.

The MSR Action3D dataset contains 557 depth video samples of 20 actions from 10 subjects. Each action is performed 2 or 3 times by every subject. We adopt the same cross-subject settings in [54], where all the 20 actions were employed. Half of the subjects are used for training and the rest for testing.

The UTD-MHAD dataset is composed of 861 depth video samples for 27 actions performed by 8 subjects. Every subject performs each action 4 times. We adopt the same experimental settings in [55], where the 27 actions were employed. Half of the subjects were used for training and the other half for testing.

### B. Implementation details

Each depth frame is converted to a point cloud set using the public code provided by 3DV-PointNet++. We sample 512 points from the point cloud set as a point cloud frame. Specifically, we first randomly sample 2048 points from the point cloud set. Then, 512 points are chosen from the 2048 points using the PFS algorithm. In the hyperpoint embedding module, the set abstraction operation is performed twice on each point cloud frame to model spatial structures. In the first set abstraction operation, 128 centroids are chosen to determine point groups. The group radius is set to 0.06. The point number in each point group is set to 48. In the second set abstraction operation, 32 centroids are chosen to determine point groups. The group radius is set to 0.1. The point number in each point group is set to 16. In the Hyperpoint-Mixer module, the number of space dislocation layers is set to 2. The same data augmentation strategies in 3DV-PointNet++ are adopted on training data, including random rotation around Y and X axis, jittering, and random points dropout. We apply Adam as the optimizer. The batch size is set to 32. The learning rate begins with 0.001 and decays with a rate of 0.5 every 10 epochs. Training will end when reaching 90 epochs.

**Details on the network architecture.** We provide the details of SequentialPointNet as follows. In the hyperpoint embedding module, three sets of MLPs are used (*i.e.*, two sets of MLPs are used in two set abstraction operations and another set of MLPs are used in the finally PointNet layer). Each set of MLPs includes three MLPs. The out channels of the first set of MLPs are set as 64, 64, and 128, respectively. The out channels of the second set of MLPs are set as 128, 128, and 256, respectively. The out channels of the third set of MLPs are set as 256, 512, and 1024, respectively. In the Hyperpoint-Mixer module, two sets of MLPs are used in two space dislocation layers. Each set of MLPs includes one MLP of 1024 out channels. The output channels of the fully-connected classifier head are set as 256 and the number of action categories.

### C. Comparison with the state-of-the-art methods

In this section, in order to verify the recognition accuracy of our SequentialPointNet, comparison experiments with other state-of-the-art approaches are implemented on NTU RGB+D

60 dataset, NTU RGB+D 120 dataset, MSR Action3D dataset, and UTD-MHAD dataset.

1) *NTU RGB+D 60 dataset:* We first compare our SequentialPointNet with the state-of-the-art methods on the NTU RGB+D 60 dataset. The NTU RGB+D 60 dataset is a large-scale indoor human action dataset. As indicated in Table I, SequentialPointNet achieves 90.3% and 97.6% on the cross-subject and cross-view test settings, respectively. Although there is a small gap between our method and skeleton sequence-based DDGCN on the cross-subject test setting, SequentialPointNet surpasses DDGCN by 0.5% on the cross-view test setting. Compared with depth sequences and point cloud sequences, skeleton sequences have the point tracking nature which is convenient for exploring fine temporal information. Fine temporal information mitigates the effect of subject diversity on action recognition, achieving higher recognition accuracy on the cross-subject test setting. It is worth mentioning that SequentialPointNet shows strong performance on par or even better than other point sequence-based approaches. Our SequentialPointNet achieves state-of-the-art performance among all methods on the cross-view test setting and results in similar recognition accuracy as PSTNet on the cross-subject test setting. The key success of our SequentialPointNet lies in effectively capturing human appearance information from each point cloud frame by the hyperpoint embedding module and the channel-mix layer in the Hyperpoint-Mixer module. Separating the channel-mixing operations and the frame-mixing operation avoids the mutual influence of spatial and temporal information extraction, which maximizes the human appearance encoding ability. Moreover, the symmetry function assisted by the hyperpoint dislocation block also preserves plentiful temporal information for effective human action recognition.

TABLE I  
ACTION RECOGNITION ACCURACY (%) ON NTU RGB+D 60

Method/Year	Input	Cross-subject	Cross-view
Wang <i>et al.</i> (2018) [56]	depth	87.1	84.2
MVDI(2019) [57]	depth	84.6	87.3
3DFCNN(2020) [58]	depth	78.1	80.4
Stateful ConvLSTM(2020) [59]	depth	80.4	79.9
ST-GCN(2018) [60]	skeleton	81.5	88.3
AS-GCN(2019) [61]	skeleton	86.8	94.2
2s-AGCN(2019) [62]	skeleton	88.5	95.1
DGNN(2019) [63]	skeleton	89.9	96.1
DDGCN(2020) [64]	skeleton	<b>91.1</b>	97.1
3s-CrosSCLR(2021) [65]	skeleton	86.2	92.5
Sym-GNN(2021) [66]	skeleton	90.1	96.4
3DV-PointNet++(2020) [49]	point	88.8	96.3
P4Transformer(2021) [18]	point	90.2	96.4
PSTNet(2021) [17]	point	90.5	96.5
SequentialPointNet(ours)	point	90.3	<b>97.6</b>

2) *NTU RGB+D 120 dataset:* We then compare our SequentialPointNet with the state-of-the-art methods on the NTU RGB+D 120 dataset. The NTU RGB+D 120 dataset is the

largest dataset for 3D action recognition. Compared with NTU RGB+D 60 dataset, it is more challenging to perform 3D human motion recognition on the NTU RGB+D 120 dataset. As indicated in Table II, SequentialPointNet achieves 83.5% and 95.4% on the cross-subject and cross-setup test settings, respectively. Note that, even on the largest human action dataset, SequentialPointNet still gains a strong lead on the cross-setup test setting among all 3D human action recognition methods and achieves state-of-the-art performance. Compared with the state-of-the-art method, SequentialPointNet does not show a competitive recognition accuracy on the cross-subject setting. There is a gap between our method and PSTNet, which is due to the loss of fine temporal changes. Fine temporal changes mitigate the effect of subject diversity on the performance of action recognition. However, a small loss of temporal information is a necessary concession to frame-level parallelism.

TABLE II  
ACTION RECOGNITION ACCURACY (%) ON NTU RGB+D 120

Method/Year	Input	Cross-subject	Cross-setup
Baseline(2018) [53]	depth	48.7	40.1
ST-GCN(2018) [60]	skeleton	81.5	88.3
MS-G3D Net (2020) [67]	skeleton	86.9	88.4
4s Shift-GCN(2020) [68]	skeleton	85.9	87.6
SGN(2020) [69]	skeleton	79.2	81.5
3s-CrosSCLR(2021) [65]	skeleton	80.5	80.4
3DV-PointNet++(2020) [49]	point	82.4	93.5
P4Transformer(2021) [18]	point	86.4	93.5
PSTNet(2021) [17]	point	<b>87.0</b>	93.5
SequentialPointNet(ours)	point	83.5	<b>95.4</b>

3) *MSR Action3D dataset*: In order to comprehensively evaluate our method, comparative experiments are also carried out on the small-scale MSR Action3D dataset. In order to alleviate the overfitting problem on the small-scale dataset, the batch size is set as 16. Other parameter settings remain the same as those on the two large-scale datasets. Table III illustrates the recognition accuracy of different methods when using different numbers of point cloud frames. It's interesting to see that, as the number of point cloud frames increases, the recognition accuracy of our method increases faster than MeteorNet, P4Transformer, and PSTNet. When using 24 point cloud frames as inputs, our model achieved state-of-the-art performance on the MSR Action3D dataset.

4) *UTD-MHAD dataset*: We evaluate our method on another small-scale UTD-MHAD dataset. The batch size is set as 16. Other parameter settings remain the same as those on the two large-scale datasets. SequentialPointNet is the first point cloud sequence model conducted on the UTD-MHAD dataset. In this paper, point cloud sequences are converted from depth sequences. To verify the recognition performance of SequentialPointNet, we compare the proposed approach with other depth sequence-based methods. Table IV illustrates the recognition accuracy of different methods. SequentialPointNet has the highest recognition accuracy of 92.31%. Experimental

TABLE III  
ACTION RECOGNITION ACCURACY (%) ON MSR-ACTION3D

Method/Year	Input	# Frames	Accuracy
Kläser <i>et al.</i> (2008) [70]	depth	18	81.43
Vieira <i>et al.</i> (2012) [71]	depth	20	78.20
Actionlet(2012) [72]	skeleton	all	88.21
		4	78.11
		8	81.14
MeteorNet(2019) [16]	point	12	86.53
		16	88.21
		24	88.50
PointNet++(2020) [15]	point	1	61.61
		4	80.13
		8	83.17
P4Transformer(2021) [18]	point	12	87.54
		16	89.56
		20	90.24
		24	90.94
		4	81.14
		8	83.50
PSTNet(2021) [17]	point	12	87.88
		16	89.90
		24	91.20
		4	77.66
		8	86.45
SequentialPointNet(ours)	point	12	88.64
		16	89.56
		20	91.21
		24	<b>91.94</b>

results on two small-scale datasets demonstrate that our approach can achieve superior recognition accuracy even without a large amount of data for training.

TABLE IV  
ACTION RECOGNITION ACCURACY (%) ON UTD-MHAD

Method/Year	Input	Accuracy
3DHOT-MBC(2017) [73]	depth	84.40
HP-DMM-CNN(2018) [74]	depth	82.75
DMI-CNN(2018) [75]	depth	50.00
HP-DMM(2018) [76]	depth	73.72
Yang <i>et al.</i> (2020) [77]	depth	88.37
Trelinski <i>et al.</i> (2021) [78]	depth	88.14
DRDIS(2021) [79]	depth	87.88
SequentialPointNet(ours)	point	<b>92.31</b>

#### D. Ablation study

In this section, comprehensive ablation studies are performed on NTU RGB+D 60 dataset to validate the contributions of different components in our SequentialPointNet.

1) *Effectiveness of Hyperpoint-Mixer module:* We conduct the experiments to demonstrate the effectiveness of the Hyperpoint-Mixer module, and results are reported in Table V. In order to prove modeling ability of this module to hyperpoint sequences, several strong deep networks are used to instead of the Hyperpoint-Mixer module in our SequentialPointNet. In SequentialPointNet (LSTM), LSTM is employed. In SequentialPointNet (GRU), GRU is employed. In SequentialPointNet (Transformer), a Transformer of two attention layers is used. In SequentialPointNet (MLP-Mixer), a MLP-Mixer of two mixer layers is used.

We can see from the table that results of SequentialPointNet (LSTM), SequentialPointNet (GRU), and SequentialPointNet (Transformer) are much worse when compared with the result of SequentialPointNet. Internal structures of hyperpoints generate the main discriminant information and the changes between hyperpoints are auxiliary. Therefore, recurrent models that implement strict temporal inference are not suitable for hyperpoint sequences. Recently, self-attention-based Transformer has remained dominant in natural language processing and computer vision [80]. Transformer is expected to achieve superior performance on the hyperpoint sequence classification task. However, due to the lack of larger-scale data for pre-training, Transformer does not show a promising result. SequentialPointNet (MLP-Mixer) achieves the accuracy of 94.5%, which is 3.1% lower than our SequentialPointNet. In MLP-Mixer, channel-mixing and token-mixing are performed alternately, resulting in the mutual influence of spatial and temporal information extraction.

TABLE V  
CROSS-VIEW RECOGNITION ACCURACY (%) WHEN USING MODELS ON  
THE NTU RGB+D 60 DATASET

Method	Accuracy
SequentialPointNet(LSTM)	85.9
SequentialPointNet(GRU)	86.4
SequentialPointNet(Transformer)	81.6
SequentialPointNet(MLP-Mixer)	94.5
SequentialPointNet	97.6

2) *Different temporal information embedding manners:* To demonstrate the effectiveness of the hyperpoint dislocation block in the Hyperpoint-Mixer module, we also report the results of SequentialPointNet (4D, w/o hdb), which does not use the hyperpoint dislocation block and injects the order information by appending the 1D temporal dimension to raw 3D points in each point cloud frame. Results are tabulated in Table VI. From the table, we observe that SequentialPointNet with the hyperpoint dislocation block outperforms SequentialPointNet (4D, w/o hdb). Therefore, the temporal information embedding manner used in SequentialPointNet is more efficient. From the experimental results, we can draw a conclusion that premature embedding of temporal information will affect spatial information encoding and reduce the accuracy of human action recognition.

3) *Effectiveness of multi-level feature learning in the Hyperpoint-Mixer module:* With the stacking of the space

TABLE VI  
CROSS-VIEW RECOGNITION ACCURACY (%) OF DIFFERENT METHODS ON  
THE NTU RGB+D 60 DATASET

Method	Accuracy
SequentialPointNet(4D, w/o hdb)	95.4
SequentialPointNet(w/o mfl)	96.9
SequentialPointNet(w/o apn)	97.1
SequentialPointNet	97.6

dislocation layer in the Hyperpoint-Mixer module, hyperpoints are dislocated at increasingly larger scales. In the larger dislocation space, the coordinates of hyperpoints record more temporal information but less spatial information. In order to obtain more discriminant information, multi-level features from different dislocation spaces are added by skip-connection operations. To verify the effectiveness of the multi-level feature learning, we report the result of SequentialPointNet (w/o mfl) that classify human actions without the multi-level features. We can see from Table VI that the recognition accuracy of SequentialPointNet (w/o mfl) decreases by 0.7% without the multi-level feature learning.

4) *Effectiveness of Augmentation PointNet layer:* We design the augmentation PointNet layer in set abstract operations of the hyperpoint embedding module to encode the spatial structures of human actions. There are two main improvements. First, we used the distance between each local point and the corresponding centroid as a 1-dim additional point feature to alleviate the influence of rotational motion on action recognition. Second, the inter-feature attention mechanism is used to optimize the fusion effect of different features. In order to verify the effectiveness of the augmentation PointNet layer, we report the result of SequentialPointNet (w/o apn) that classifies human actions without the augmentation PointNet layer. From Table VI, we observe that the recognition accuracy of SequentialPointNet with the augmentation PointNet layer increases by 0.5% than SequentialPointNet (w/o apn).

5) *Results of our SequentialPointNet when setting different layers of pyramids in the hierarchical pyramid max pooling operation:* To investigate the choice of the number of the pyramid layers in the hierarchical pyramid max pooling operation, we compare the performance of our SequentialPointNet with the different numbers of pyramid layers. The hierarchical pyramid max pooling operation is used as the frame-mixing operation to mix the dynamic information within subactions. Too few layers of the pyramid cannot obtain enough temporal multi-scale information of human motion. Too many layers of the pyramid tend to introduce redundant information and increase computational costs. The results are presented in Fig. 7. Particularly, the 2-layer pyramid is the optimal choice for SequentialPointNet.

6) *Results of our SequentialPointNet when using different numbers of point cloud frames:* We also investigate the performance variation of our method when using different numbers of point cloud frames. As shown in Fig. 8, better performance is gained when the number of point cloud frames increases. When the number of frames is greater than 20, the

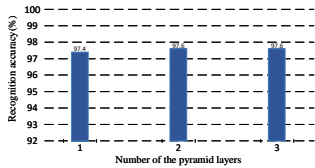


Fig. 7. Cross-view recognition accuracy (%) of our SequentialPointNet when using different numbers of pyramid layers on the NTU RGB+D 60 dataset.

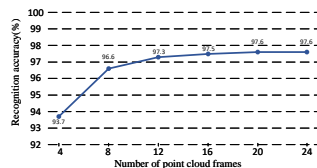


Fig. 8. Cross-view recognition accuracy (%) of our SequentialPointNet when using different numbers of frames on the NTU RGB+D 60 dataset.

recognition accuracy tends to stabilize. Therefore, the number of the point cloud frames is set to 20.

### E. Memory usage and computational efficiency

In this section, we evaluate the memory usage, computational efficiency and parallelism of our method. Experiments are conducted on the machine with one Intel(R) Xeon(R) W-3175X CPU and one Nvidia RTX 3090 GPU. In Table VII, the number of parameters, the number of floating point operations (FLOPs), and the running time of our SequentialPointNet are compared with MeteorNet, 3DV-PointNet++, P4Transformer, and PSTNet. The running time is the network forward inference time per point cloud sequence and counted in the same way as 3DV-PointNet++. FLOPs of MeteorNet, P4Transformer, and PSTNet are not provided by their authors.

TABLE VII  
PARAMETERS, FLOATING POINT OPERATIONS, AND RUNNING TIMES  
COMPARISON OF DIFFERENT METHODS

Method	Parameters (M)	FLOPs (G)	Time (ms)
MeteorNet [16]	17.60	-	56.49
3DV-PointNet++ [49]	<b>1.24</b>	<b>1.24</b>	54
P4Transformer [18]	44.1	-	96.48
PSTNet [17]	20.46	-	106.35
SequentialPointNet	3.72	2.84	<b>5</b>

From the table, we can see that parameters in 3DV-PointNet++ are the fewest in all methods. This is because 3DV-PointNet++ converts point cloud sequences to 3D point clouds, and employs static point cloud methods to process 3D point clouds. Compared with point cloud sequence methods, the static point cloud method has fewer parameters but lower recognition accuracy. It is noticed from the table that only our SequentialPointNet has a similar number of parameters as 3DV-PointNet++. The parameter number of SequentialPointNet is much less than MeteorNet, P4Transformer, and PSTNet, which verifies that our approach is the most lightweight point cloud sequence model. In addition, SequentialPointNet is far faster than other methods, even though 3DV-PointNet++ has fewer FLOPs. SequentialPointNet takes only 5 milliseconds to classify a point cloud sequence. In 3DV-PointNet++, a multi-stream 3D action recognition manner is proposed to learn motion and appearance features jointly. However, the multi-stream manner limits the parallelism of 3DV-PointNet++. In

MeteorNet, P4Transformer, and PSTNet, Cross-frame spatio-temporal local neighborhoods are constructed, which is time-consuming and not conducive to parallel computing. SequentialPointNet improves the speed of modeling point cloud sequences by more than 10 times. The superior computational efficiency of our SequentialPointNet is due to the lightweight network architecture and strong frame-level parallelism.

Since there is no computational dependency, in the case of limited computing power, frame-level units can also be deployed on different devices or executed sequentially on a single device.

## V. CONCLUSION

In this paper, we have proposed a strong frame-level parallel point cloud sequence network referred to as SequentialPointNet for 3D action recognition, which greatly improves the efficiency of modeling point cloud sequences. SequentialPointNet is composed of two serial modules, *i.e.*, a hyperpoint embedding module and a Hyperpoint-Mixer module. First, each point cloud frame is flattened into a hyperpoint by the same trainable hyperpoint embedding module. Then, we input the hyperpoint sequence into the Hyperpoint-Mixer module to perform feature mixing operations. In the Hyperpoint-Mixer module, channel-mixing operations and frame-mixing operations are clearly separated and the frame-mixing operation is placed at the end of all operations. By doing so, the main operations of SequentialPointNet can be divided into frame-level units executed in parallel. Extensive experiments conducted on four public datasets show that SequentialPointNet has the fastest computation speed and superior recognition performance among all point cloud sequence models.

## REFERENCES

- [1] W. Zhu, C. Lan, J. Xing, W. Zeng, Y. Li, L. Shen, and X. Xie, "Co-occurrence feature learning for skeleton based action recognition using regularized deep lstm networks," *Proceedings of the AAAI conference on artificial intelligence*, 2016.
- [2] J. Liu, A. Shahroudy, D. Xu, A. C. Kot, and G. Wang, "Skeleton-based action recognition using spatio-temporal lstm network with trust gates," *IEEE transactions on pattern analysis and machine intelligence*, vol. 40, no. 12, 2018.
- [3] S. Zhang, X. Liu, and J. Xiao, "On geometric features for skeleton-based action recognition using multilayer lstm networks," *2017 IEEE Winter Conference on Applications of Computer Vision*, 2017.
- [4] C. Li, Q. Zhong, D. Xie, and S. Pu, "Co-occurrence feature learning from skeleton data for action recognition and detection with hierarchical aggregation," *arXiv preprint arXiv:1804.06055*, 2018.
- [5] Y. Li, R. Xia, X. Liu, and Q. Huang, "Learning shape-motion representations from geometric algebra spatio-temporal model for skeleton-based action recognition," *2019 IEEE International Conference on Multimedia and Expo*, 2019.
- [6] P. Wang, W. Li, Z. Gao, J. Zhang, C. Tang, and P. O. Ogunbona, "Action recognition from depth maps using deep convolutional neural networks," *IEEE Transactions on Human-Machine Systems*, 2015.
- [7] P. Wang, S. Wang, Z. Gao, Y. Hou, and W. Li, "Structured images for rgb-d action recognition," *Proceedings of the IEEE International Conference on Computer Vision Workshops*, 2017.
- [8] M. Harville and D. Li, "Fast, integrated person tracking and activity recognition with plan-view templates from a single stereo camera," *Proceedings of the IEEE/CVF conference on computer vision and pattern recognition*, 2004.
- [9] M.-C. Roh, H.-K. Shin, and S.-W. Lee, "View-independent human action recognition with volume motion template on single stereo camera," *Pattern Recognition Letters*, 2010.

- [10] X. Yang, C. Zhang, and Y. Tian, "Recognizing actions using depth motion maps-based histograms of oriented gradients," *Proceedings of the 20th ACM international conference on Multimedia*, 2012.
- [11] H. Rahmani and A. Mian, "3d action recognition from novel viewpoints," *Proceedings of the IEEE/CVF conference on computer vision and pattern recognition*, 2016.
- [12] Y. Min, Y. Zhang, X. Chai, and X. Chen, "An efficient pointlstm for point clouds based gesture recognition," *Proceedings of the IEEE/CVF conference on computer vision and pattern recognition*, 2020.
- [13] G. Wang, H. Liu, M. Chen, Y. Yang, Z. Liu, and H. Wang, "Anchor-based spatial-temporal attention convolutional networks for dynamic 3d point cloud sequences," *arXiv preprint arXiv:2012.10860*, 2020.
- [14] H. Wang, L. Yang, X. Rong, J. Feng, and Y. Tian, "Self-supervised 4d spatio-temporal feature learning via order prediction of sequential point cloud clips," *Proceedings of the IEEE/CVF Winter Conference on Applications of Computer Vision*, 2021.
- [15] C. R. Qi, L. Yi, H. Su, and L. J. Guibas, "Pointnet++: Deep hierarchical feature learning on point sets in a metric space," *Advances in Neural Information Processing Systems*, 2017.
- [16] X. Liu, M. Yan, and J. Bohg, "MeteorNet: Deep Learning on Dynamic 3D Point Cloud Sequences," *Proceedings of the IEEE International Conference on Computer Vision*, 2019.
- [17] H. Fan, X. Yu, Y. Ding, Y. Yang, and M. Kankanhalli, "Pstnet: Point spatio-temporal convolution on point cloud sequences," *International Conference on Learning Representations*, 2021.
- [18] H. Fan, Y. Yang, and M. Kankanhalli, "Point 4d transformer networks for spatio-temporal modeling in point cloud videos," *Proceedings of the IEEE/CVF Conference on Computer Vision and Pattern Recognition*, 2021.
- [19] H. Su, S. Maji, E. Kalogerakis, and E. Learned-Miller, "Multi-view convolutional neural networks for 3D shape recognition," *Proceedings of the IEEE international conference on computer vision*, 2015.
- [20] T. Yu, J. Meng, and J. Yuan, "Multi-view harmonized bilinear network for 3D object recognition," *Proceedings of the IEEE/CVF conference on computer vision and pattern recognition*, 2018. Z. Yang and L. Wang, "Learning relationships for multi-view 3D object recognition," *Proceedings of the IEEE international conference on computer vision*, 2019.
- [21] C. R. Qi, H. Su, M. Nießner, A. Dai, M. Yan, and L. J. Guibas, "Volumetric and multi-view CNNs for object classification on 3D data," *Proceedings of the IEEE/CVF conference on computer vision and pattern recognition*, 2016.
- [22] Y. Feng, Z. Zhang, X. Zhao, R. Ji, and Y. Gao, "GVCNN: Group-view convolutional neural networks for 3D shape recognition," *Proceedings of the IEEE/CVF conference on computer vision and pattern recognition*, 2018.
- [23] C. Ma, Y. Guo, J. Yang, and W. An, "Learning multi-view representation with LSTM for 3D shape recognition and retrieval," *IEEE Transactions on Multimedia*, 2018.
- [24] Z. Wang and F. Lu, "VoxSegNet: Volumetric CNNs for semantic part segmentation of 3D shapes," *IEEE transactions on visualization and computer graphics*, 2019.
- [25] E. Kalogerakis, M. Averkiou, S. Maji, and S. Chaudhuri, "3D shape segmentation with projective convolutional networks," *Proceedings of the IEEE/CVF conference on computer vision and pattern recognition*, 2017.
- [26] L. Yi, H. Su, X. Guo, and L. J. Guibas, "SyncSpecCNN: Synchronized spectral CNN for 3D shape segmentation," *Proceedings of the IEEE/CVF conference on computer vision and pattern recognition*, 2017.
- [27] P. Wang, Y. Gan, P. Shui, F. Yu, Y. Zhang, S. Chen, and Z. Sun, "3D shape segmentation via shape fully convolutional networks," *Computers & Graphics*, 2018.
- [28] C. Zhu, K. Xu, S. Chaudhuri, L. Yi, L. Guibas, and H. Zhang, "CoSegNet: Deep co-segmentation of 3D shapes with group consistency loss," *arXiv preprint arXiv:1903.10297*, 2019.
- [29] I. Armeni, O. Sener, A. R. Zamir, H. Jiang, I. Brilakis, M. Fischer, and S. Savarese, "3D semantic parsing of large-scale indoor spaces," *Proceedings of the IEEE/CVF conference on computer vision and pattern recognition*, 2016.
- [30] F. Liu, S. Li, L. Zhang, C. Zhou, R. Ye, Y. Wang, and J. Lu, "3DCNN-DQN-RNN: A deep reinforcement learning framework for semantic parsing of large-scale 3D point clouds," *Proceedings of the IEEE international conference on computer vision*, 2017.
- [31] Z. Wu, S. Song, A. Khosla, F. Yu, L. Zhang, X. Tang, and J. Xiao, "3D shapeNets: A deep representation for volumetric shapes," *Proceedings of the IEEE/CVF conference on computer vision and pattern recognition*, 2015.
- [32] D. Maturana and S. Scherer, "VoxNet: A 3D convolutional neural network for real-time object recognition," 2015 IEEE/RSJ International Conference on Intelligent Robots and Systems, 2015.
- [33] G. Riegler, A. Osman Ulusoy, and A. Geiger, "OctNet: Learning deep 3D representations at high resolutions," *Proceedings of the IEEE/CVF conference on computer vision and pattern recognition*, 2017.
- [34] P.-S. Wang, Y. Liu, Y.-X. Guo, C.-Y. Sun, and X. Tong, "O-CNN: Octree-based convolutional neural networks for 3D shape analysis," *ACM Transactions On Graphics*, 2017.
- [35] T. Le and Y. Duan, "PointGrid: A deep network for 3D shape understanding," *Proceedings of the IEEE/CVF conference on computer vision and pattern recognition*, 2018.
- [36] Y. Ben-Shabat, M. Lindenbaum, and A. Fischer, "3D point cloud classification and segmentation using 3D modified fisher vector representation for convolutional neural networks," *arXiv preprint arXiv:1711.08241*, 2017.
- [37] M. Joseph-Rivlin, A. Zvirin, and R. Kimmel, "Mo-Net: Flavor the moments in learning to classify shapes," *Proceedings of the IEEE international conference on computer vision*, 2018.
- [38] J. Yang, Q. Zhang, B. Ni, L. Li, J. Liu, M. Zhou, and Q. Tian, "Modeling point clouds with self-attention and gumbel subset sampling," *Proceedings of the IEEE/CVF conference on computer vision and pattern recognition*, 2019.
- [39] H. Zhao, L. Jiang, C.-W. Fu, and J. Jia, "PointWeb: Enhancing local neighborhood features for point cloud processing," *Proceedings of the IEEE/CVF conference on computer vision and pattern recognition*, 2019.
- [40] Y. Duan, Y. Zheng, J. Lu, J. Zhou, and Q. Tian, "Structural relational reasoning of point clouds," *Proceedings of the IEEE/CVF conference on computer vision and pattern recognition*, 2019.
- [41] C. R. Qi, H. Su, K. Mo, and L. J. Guibas, "PointNet: Deep learning on point sets for 3D classification and segmentation," *Proceedings of the IEEE/CVF conference on computer vision and pattern recognition*, 2017.
- [42] K. M. Hermann, T. Kocisky, E. Grefenstette, L. Espeholt, W. Kay, M. Suleyman, and P. Blunsom, "Teaching machines to read and comprehend," *Advances in neural information processing systems*, 2015.
- [43] R. Jozefowicz, W. Zaremba, and I. Sutskever, "An empirical exploration of recurrent network architectures," *International conference on machine learning*, 2015.
- [44] J. Donahue, L. Anne Hendricks, S. Guadarrama, M. Rohrbach, S. Venugopalan, K. Saenko, and T. Darrell, "Long-term recurrent convolutional networks for visual recognition and description," *Proceedings of the IEEE/CVF Conference on Computer Vision and Pattern Recognition*, 2015.
- [45] W. Du, Y. Wang, and Y. Qiao, "Rpan: An end-to-end recurrent pose-attention network for action recognition in videos," *Proceedings of the IEEE International Conference on Computer Vision*, 2017.
- [46] S. Hochreiter, and J. Schmidhuber, "Long short-term memory," *Neural computation*, 1997.
- [47] J. Chung, C. Gulcehre, K. Cho, and Y. Bengio, "Empirical evaluation of gated recurrent neural networks on sequence modeling," *arXiv preprint arXiv:1412.3555*, 2014.
- [48] A. Vaswani, N. Shazeer, N. Parmar, J. Uszkoreit, L. Jones, A. N. Gomez, and I. Polosukhin, "Attention is all you need" In *Advances in neural information processing systems*, 2017.
- [49] Y. Wang, Y. Xiao, F. Xiong, W. Jiang, Z. Cao, J. T. Zhou, and J. Yuan, "3dv: 3d dynamic voxel for action recognition in depth video," *Proceedings of the IEEE/CVF Conference on Computer Vision and Pattern Recognition*, 2020.
- [50] S. Woo, J. Park, J. Y. Lee, and I. S. Kweon, "Cbam: Convolutional block attention module," *Proceedings of the European conference on computer vision*, 2018.
- [51] H. Ding, X. Jiang, and B. Shuai, "Context contrasted feature and gated multi-scale aggregation for scene segmentation," *Proceedings of the IEEE Conference on Computer Vision and Pattern Recognition*, 2018.
- [52] A. Shahroudy, J. Liu, T.-T. Ng, and G. Wang, "Ntu rgb+d: A large scale dataset for 3d human activity analysis," *Proceedings of the IEEE/CVF conference on computer vision and pattern recognition*, 2016.
- [53] J. Liu, A. Shahroudy, M. Perez, G. Wang, L. Yüduan, and A. C. Kot, "NTU RGB+D 120: A largescale benchmark for 3d human activity understanding," *IEEE transactions on pattern analysis and machine intelligence*, 2020.
- [54] W. Li, Z. Zhang, and Z. Liu, "Action recognition based on a bag of 3d points," *Proceedings of the IEEE/CVF conference on computer vision and pattern recognition*, 2010.

- [55] C. Chen, R. Jafari, and N. Kehtarnavaz, "UTD-MHAD: A multimodal dataset for human action recognition utilizing a depth camera and a wearable inertial sensor," *IEEE International conference on image processing*, 2015.
- [56] P. Wang, W. Li, Z. Gao, C. Tang, and P. O. Ogunbona, "Depth pooling based large-scale 3-d action recognition with convolutional neural networks," *IEEE Transactions on Multimedia*, vol. 20, no. 5, 2018.
- [57] Y. Xiao, J. Chen, Y. Wang, Z. Cao, J. T. Zhou, and X. Bai, "Action recognition for depth video using multi-view dynamic images," *Information Sciences*, vol. 480, 2019.
- [58] A. Sanchez-Caballero, S. de López-Diz, D. Fuentes-Jimenez, C. Losada-Gutiérrez, M. Marrón-Romera, D. Casillas-Perez, and M. I. Sarker, "3dfcnn: Real-time action recognition using 3d deep neural networks with raw depth information," *arXiv preprint arXiv:2006.07743*, 2020.
- [59] A. Sanchez-Caballero, D. Fuentes-Jimenez, and C. Losada-Gutierrez, "Exploiting the convlstm: Human action recognition using raw depth video-based recurrent neural networks," *arXiv preprint arXiv:2006.07744*, 2020.
- [60] S. Yan, Y. Xiong, and D. Lin, "Spatial temporal graph convolutional networks for skeleton-based action recognition," *Thirty-second AAAI conference on artificial intelligence*, 2018.
- [61] M. Li, S. Chen, X. Chen, Y. Zhang, Y. Wang, and Q. Tian, "Action-structural graph convolutional networks for skeleton-based action recognition," *Proceedings of the IEEE/CVF conference on computer vision and pattern recognition*, 2019.
- [62] L. Shi, Y. Zhang, J. Cheng, and H. Lu, "Two-stream adaptive graph convolutional networks for skeleton-based action recognition," *Proceedings of the IEEE/CVF conference on computer vision and pattern recognition*, 2019.
- [63] L. Shi, Y. Zhang, J. Cheng, and H. Lu, "Skeleton-based action recognition with directed graph neural networks," *Proceedings of the IEEE/CVF Conference on Computer Vision and Pattern Recognition*, 2019.
- [64] M. Korban and X. Li, "Ddgc: A dynamic directed graph convolutional network for action recognition," *European Conference on Computer Vision*, 2020.
- [65] L. Li, M. Wang, B. Ni, H. Wang, J. Yang, and W. Zhang, "3d human action representation learning via cross-view consistency pursuit," *Proceedings of the IEEE/CVF Conference on Computer Vision and Pattern Recognition*, 2021.
- [66] M. Li, S. Chen, X. Chen, Y. Zhang, Y. Wang, and Q. Tian, "Symbiotic graph neural networks for 3d skeleton-based human action recognition and motion prediction," *IEEE Transactions on Pattern Analysis and Machine Intelligence*, 2021.
- [67] Z. Liu, H. Zhang, Z. Chen, Z. Wang, and W. Ouyang, "Disentangling and unifying graph convolutions for skeleton-based action recognition," *Proceedings of the IEEE/CVF Conference on Computer Vision and Pattern Recognition*, 2020.
- [68] K. Cheng, Y. Zhang, X. He, W. Chen, J. Cheng, and H. Lu, "Skeleton-based action recognition with shift graph convolutional network," *Proceedings of the IEEE/CVF Conference on Computer Vision and Pattern Recognition*, 2020.
- [69] P. Zhang, C. Lan, W. Zeng, J. Xing, J. Xue, and N. Zheng, "Semantics-guided neural networks for efficient skeleton-based human action recognition," *Proceedings of the IEEE/CVF Conference on Computer Vision and Pattern Recognition*, 2020.
- [70] A. Kläser, M. Marszałek, and C. Schmid, "A spatio-temporal descriptor based on 3d-gradients," *BMVC 2008-19th British Machine Vision Conference British Machine Vision Association*, 2008.
- [71] W. A. Vieira, E. R. Nascimento, G. L. Oliveira, Z. Liu, and M. F. Campos, "Stop: Space-time occupancy patterns for 3d action recognition from depth map sequences," *Iberoamerican congress on pattern recognition*, Springer, Berlin, Heidelberg, 2012.
- [72] J. Wang, Z. Liu, Y. Wu, and J. Yuan, "Mining actionlet ensemble for action recognition with depth cameras," *Proceedings of the IEEE/CVF Conference on Computer Vision and Pattern Recognition*, 2012.
- [73] B. Zhang, Y. Yang, C. Chen, L. Yang, and L. Han, "Action recognition using 3D histograms of texture and a multi-class boosting classifier," *IEEE Transactions on Image processing*, 2017.
- [74] N. E. D. Elmadany, Y. He, and L. Guan, "Information fusion for human action recognition via biset/multiset globality locality preserving canonical correlation analysis," *IEEE Transactions on Image Processing*, 2018.
- [75] A. Kamel, B. Sheng, and P. Yang, "Deep convolutional neural networks for human action recognition using depth maps and postures," *IEEE Transactions on Systems, Man, and Cybernetics: Systems*, 2018.
- [76] N. E. D. Elmadany, Y. He, and L. Guan, "Multimodal learning for human action recognition via bimodal/multimodal hybrid centroid canonical correlation analysis," *IEEE Transactions on Multimedia*, 2018.
- [77] T. Yang, Z. Hou, and J. Liang, "Depth sequential information entropy maps and multi-label subspace learning for human action recognition," *IEEE Access*, 2020.
- [78] J. Trelinski, and B. Kwalek, "CNN-based and DTW features for human activity recognition on depth maps," *Neural Computing and Applications*, 2021.
- [79] H. Wu, X. Ma, and Y. Li, "Spatiotemporal multimodal learning with 3D CNNs for video action recognition," *IEEE Transactions on Circuits and Systems for Video Technology*, 2021.
- [80] A. Dosovitskiy, L. Beyer, and A. Kolesnikov, "An image is worth 16x16 words: Transformers for image recognition at scale," *arXiv preprint arXiv:2010.11929*, 2020.



**Xing Li** received the B.Sc. and M.Sc. degrees in software engineering from Changzhou University, China, in 2016 and 2019, respectively. He is currently pursuing the Ph.D. degree with the Department of Computer Science and Technology, Hohai University, Nanjing, China. His current research interests include machine learning, computer vision and deep learning, especially human action recognition.



**Qian Huang** received the B. Sc. degree in computer science from Nanjing University, China, in 2003, and the Ph.D. degree in computer science from the Institute of Computing Technology, Chinese Academy of Sciences, in 2010. Since Dec. 2012, he is with Hohai University, Nanjing, China, where he serves as the dean of Computer Science and Technology Department. His research interests include media computing, data mining, and intelligent education.



**Zhijian Wang** received the Ph.D. degree from Nanjing University, Nanjing, China. He is currently a Professor with Hohai University, Nanjing, China. His current research interests include machine learning, computer vision and deep learning.



**Zhenjie Hou** received the Ph.D. degree in mechanical engineering from Inner Mongolia Agricultural University, in 2005. From 1998 to 2010, he was a Professor with the Computer Science Department, Inner Mongolia Agricultural University. In August 2010, he joined Changzhou University. His research interests include signal and image processing, pattern recognition, and computer vision.



**Tianjin Yang** received the B.Sc. and M.Sc. degrees in Computer Science and Technology from Changzhou University, China, in 2018 and 2021, respectively. He is currently pursuing the Ph.D. degree with the Department of Artificial Intelligence, Hohai University, Nanjing, China. His current research interests include machine learning, computer vision.